molecular pharmaceutics

Article

pubs.acs.org/molecularpharmaceutics

Evaluation of 3,3′,4′-Trihydroxyflavone and 3,6,4′-Trihydroxyflavone (4′-*O*-Glucuronidation) as the in Vitro Functional Markers for Hepatic UGT1A1

Baojian Wu,[†] Shuxing Zhang,[‡] and Ming Hu*[,†]

[†]Department of Pharmacological and Pharmaceutical Sciences, College of Pharmacy, University of Houston, 1441 Moursund Street, Houston, Texas 77030, United States

[‡]Department of Experimental Therapeutics, The University of Texas, M. D. Anderson Cancer Center, 1515 Holcombe Blvd, Houston, Texas 77030, United States

Supporting Information

ABSTRACT: Identifying uridine 5'-diphospho-(UDP)-glucuronosyltransferase (UGT)-selective probes (substrates that are primarily glucuronidated by a single isoform) is complicated by the enzymes' large overlapping substrate specificity. Here, regioselective glucuronidation of two flavonoids, 3,3′,4′-trihydroxyflavone (3,3′,4′-THF) and 3,6,4′-trihydroxyflavone (3,6,4′-THF), is used to probe the activity of hepatic UGT1A1. The glucuronidation kinetics of 3,3′,4′-THF and 3,6,4′-THF was determined using 12 recombinant human UGT isoforms and pooled human liver microsomes (pHLM). The individual contribution of main UGT isoforms to the metabolism of the two flavonoids in pHLM was estimated using the relative activity factor approach. UGT1A1 activity correlation analyses using flavonoids-4′-*O*-glucuronidation vs *β*-estradiol-3-glucuronidation (a well-recognized marker for UGT1A1) or vs SN-38 glucuronidation were performed using a bank of HLMs (n = 12) including three UGT1A1-genotyped HLMs (i.e., UGT1A1*1*1, UGT1A1*1*28, and UGT1A1*28*28). The results showed that UGT1A1 and 1A9, followed by 1A7, were the main isoforms for glucuronidating the two flavonoids, where UGT1A1 accounted for 92 ± 7% and 91 ± 10% of 4′-*O*-glucuronidation of 3,3′,4′-THF and 3,6,4′-THF, respectively, and UGT1A9 accounted for most of the 3-*O*-glucuronidation. Highly significant correlations (R^2 > 0.944, p < 0.0001) between the rates of flavonoids 4′-*O*-glucuronidation and that of estradiol-3-glucuronidation or SN-38 glucuronidation were observed across 12 HLMs. In conclusion, UGT1A1-mediated 4′-*O*-glucuronidation of 3,3′,4′-THF and 3,6,4′-THF was highly correlated with the glucuronidation of estradiol (3-OH) and SN-38. This study demonstrated for the first time that regioselective glucuronidation of flavonoids can be applied to probe hepatic UGT1A1 activity *in vitro*.

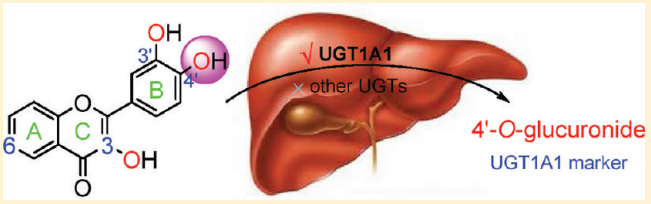

KEYWORDS: *probe substrate, flavonoids, UGTs, SN-38, regioselectivity*

INTRODUCTION

Uridine 5'-diphospho-(UDP)-glucuronosyltransferase (UGT)-mediated glucuronidation is a major phase II metabolic pathway that facilitates efficient elimination and detoxification of structurally diverse groups of xenobiotics (e.g., SN-38 and nitrosamines) and endogenous compounds (e.g., bilirubin and estradiol). UGT genetic deficiency and polymorphisms are associated with inherited physiological disorders, whereas inhibition of glucuronidation by the concomitant use of certain drugs is related to drug-induced toxicities.[1−3] On the other hand, extensive glucuronidation can be a barrier to oral bioavailability as rapid and extensive first-pass glucuronidation (or premature clearance by UGTs) of orally administered agents usually results in the poor oral bioavailability and/or lack of efficacies.[3,4]

Human UGTs are classified into four families: UGT1, UGT2, UGT3, and UGT8.[5] The most important drug-conjugating UGTs belong to UGT1 and UGT2 families. At present, 16 human UGT isoforms from UGT1A (9 members) and UGT2B (7 members) subfamilies are identified:[5] namely, UGT1A1, 1A3, 1A4, 1A5, 1A6, 1A7, 1A8, 1A9, 1A10, 2B4, 2B7, 2B10, 2B11, 2B15, 2B17, and 2B28. Their distribution (probed by mRNA level) in major metabolizing organs, as well as other organs/tissues, were well-studied.[6,7] Compared to UGT1As, UGT2Bs are much more abundantly expressed in human liver. UGT2B4 has the highest expression, followed by UGT2B15. Among the UGT1A isoforms, UGT1A1, 1A4, 1A6, and 1A9 have moderate expression in the liver.[6]

Within the nine UGT1A isoforms, UGT1A1 is perhaps the most significant one for maintaining human health. Its genetic deficiency may impair the metabolism of bilirubin, resulting in severe hyperbilirubinemia disorders such as Crigler−Najjar syndrome and Gilbert's syndrome.[1,8,9] Moreover, UGT1A1 is

Received: June 15, 2011
Revised: August 3, 2011
Accepted: October 10, 2011
Published: October 10, 2011

mainly responsible for SN-38 clearance.[10] SN-38 is the active metabolite of irinotecan (CPT-11), a widely used anticancer drug, especially for the treatment of colorectal cancer. Generic polymorphisms in UGT1A1 (e.g., UGT1A1*28 variant with low UGT1A1 expression) has been linked to irinotecan toxicity.[11] The frequency of UGT1A1*28 allele (promoter $(TA)_{6/7}TAA$ mutation) varies by ethnic and racial origin and is ~10% in a white population.[12] This high penetration rate necessitates the UGT1A1 genotyping of patients prior to the irinotecan treatment, a protocol recommended by the Food and Drug Administration (FDA).[11]

Flavonoids are a class of natural polyphenols, the consumption of which is linked to numerous health benefits such as antioxidant and anticancer.[13] It is well-known that flavonoids are subjected to extensive glucuronidation, resulting in poor oral bioavailabilities.[14,15] Although UGT1A isoforms showed vast overlapping substrate specificities (as evaluated by counting all metabolites),[16−19] regioselective glucuronidation of multihydroxyl flavonoids has been demonstrated to be highly isoform-dependent for many flavonoids.[3] In the study of quercetin glucuronidation,[20] UGT1A3's highest glucuronidation preferred 3′-*O*-glucuronide, whereas UGT1A9 favored 3-*O*-glucuronidation.

Regioselectivity refers to the preference for the formation of one glucuronide isomer over another, when a substrate possesses more than one possible glucuronidation site. The regioselectivity of various UGTs has been examined for a number of compounds such as estradiol, estrone, morphine, and resveratrol.[21−23] Elucidation of UGT regioselectivity would facilitate the understanding of UGT−substrates interaction with respect to binding properties.[24] In addition, the typical generation of a particular glucuronide isomer from a substrate was used to probe UGT activity in human tissues *in vitro*. For example, *β*-estradiol 3-glucuronidation is considered an excellent marker of UGT1A1 activity,[25,26] and morphine 6-glucuronidation may be used as a selective probe for UGT2B7 activity.[27]

As stated by Court[25] and Miners et al.,[28] UGT-selective probes have many significant applications in the study of drug glucuronidation. For example, they can be used to (1) identify a specific functional UGT in human tissues; (2) predict possible UGT-mediated drug−drug interactions; and (3) elucidate the functional significance of genetic polymorphisms. In this paper, we characterized two flavonoids (3,3′,4′-trihydroxyflavone and 3,6,4′-trihydroxyflavone) as the UGT1A1 probes based on initial screening (i.e., selectivity evaluation by phenotyping each compound with a panel of recombinant UGT isoforms) of ~67 flavonoid compounds derived from five subclasses (flavone, isoflavones, flavonone, chalcone, and flavonols) (published and unpublished data).[16−19,24,29,30] The individual contributions of UGT1A1 and/or 1A9 to metabolism of the two flavonoids and SN38 in pooled human liver microsomes were estimated using enzyme kinetic experiments combined with the relative activity factor (RAF). The selectivity of UGT1A1 toward the flavonoids, estradiol, and SN-38 were further evaluated in a bank of 12 HLMs based on activity correlation analysis.

EXPERIMENTAL SECTION

Materials. The 12 recombinant human UGT isoforms (Supersomes, i.e., UGT1A1, 1A3, 1A4, 1A6, 1A7, 1A8, 1A9, 1A10, 2B4, 2B7, 2B15, and 2B17), pooled human liver microsomes (from 50 donors), 3 UGT1A1 genotyped human liver microsomes (i.e., UGT1A1*1*1 (wild-type), UGT1A1*1*28 (allelic variant), and UGT1A1*28*28 (allelic variant)), and rabbit antihuman UGT1A1 polyclonal antibody were purchased from BD Biosciences (Woburn, MA). A bank of individual human liver microsomes with diverse UGT activities (n = 8, designated as HLM-1, HLM-2, ..., HLM-8) was purchased from Xenotech (Lenexa, KS). Rabbit antigoat IgG-HRP was purchased from Santa Cruz Biotechnology (Santa Cruz, CA). Two flavonoids (see Figure 1 for chemical structures; i.e., 3,3′,4′-trihydroxyflavone (3,3′,4′-THF), and 3,6,4′-trihydroxyflavone (3,6,4′-THF)) were purchased from Indofine Chemicals (Somerville, NJ). 17*β*-Estradiol (also referred as estradiol in this paper, see Figure 4 for chemical structure), *β*-estradiol-3-glucuronide, 7-ethyl-10-hydroxycamptothecin (SN-38, see Figure 4 for chemical structure), SN-38-glucuronide, propofol, and propofol-glucuronide were obtained from Toronto Research Chemicals (North York, Ontario, Canada). Uridine diphosphoglucuronic acid (UDPGA), alamethicin, D-saccharic-1,4-lactone monohydrate, and magnesium chloride were purchased from Sigma-Aldrich (St. Louis, MO). Ammonium acetate was purchased from J.T. Baker (Phillipsburg, NT). All other materials (typically analytical grade or better) were used as received.

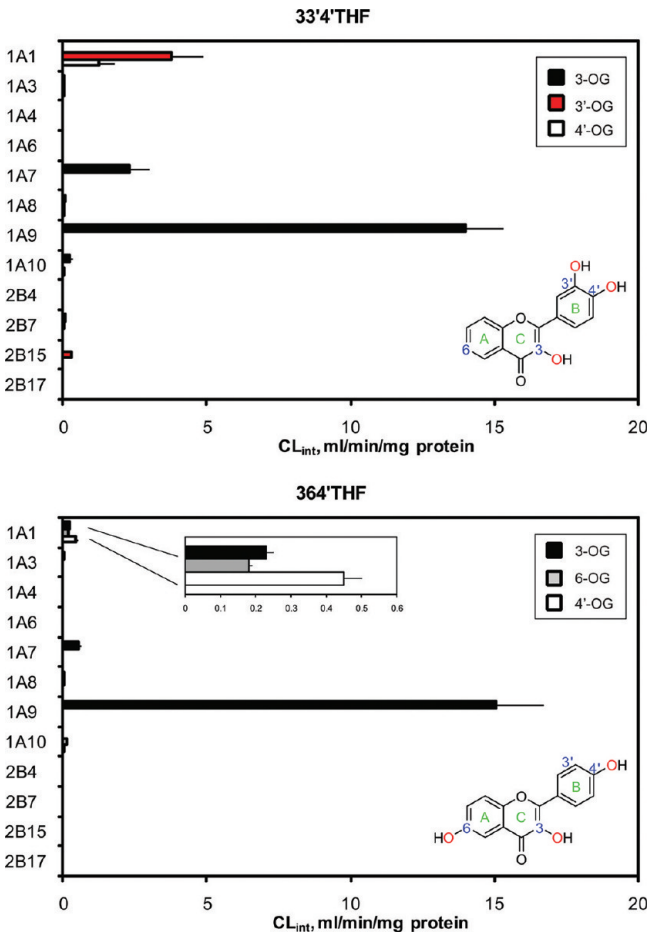

Figure 1. Phenotyping of 3,3′,4′-THF (top) and 3,6,4′-THF (bottom) using 12 recombinant UGTs, showing that UGT1A1, 1A7, and 1A9 were the main isoforms glucuronidating both flavonoids. Intrinsic clearances ($CL_{int} = V_{max}/K_m$) were obtained from kinetic determination. OG: *O*-glucuronide. Insets show corresponding chemical structures for each flavonoid probe.

Immunoblotting. The recombinant UGT1A1 and human liver microsomes were analyzed by sodium dodecyl sulfate (SDS)-polyacrylamide gel electrophoresis (10% acrylamide gels) and transferred onto PVDF membranes (Millipore, Bedford, MA). Blots were probed with anti-UGT1A1 antibody (BD Biosciences, Woburn, MA), followed by horseradish peroxidase-conjugated rabbit antigoat IgG (Santa Cruz Biotechnology, Santa Cruz, CA). Membranes were analyzed on a FluorChem FC Imaging System (Alpha Innotech), and intensities of UGT bands were measured by densitometry using the AlphaEase software.

Glucuronidation Assay and Kinetics. The experimental procedures of glucuronidation assays were exactly the same as our previous publications.[24,29,30] Glucuronide(s) formation was verified to be linear with respect to incubation time (5−60 min) and protein concentration (13−53 μg/mL). Glucuronidation rates were calculated as nanomoles of glucuronide(s) formed per reaction time per protein amount (or nmol/min/mg protein), as the actual enzyme concentration is unknown. Enzyme kinetics parameters for glucuronidation were determined by measuring initial reaction rates at a series of substrate concentrations. All experiments were performed in triplicate.

UPLC Analysis. The Waters ACQUITY UPLC (ultra performance liquid chromatography) system was used to analyze a parent compound (or aglycone) and its respective glucuronide(s). Details of the analytical conditions are given in Table S1 (Supporting Information, SI). The quantitation of estradiol-3-glucuronide, propofol glucuronide, and SN-38 glucuronide was made with the authentic reference standards, while the quantitation of the flavonoid glucuronides was based on the standard curve of the parent compound and further calibrated with the conversion factor (Table S1) using the same method that we have published earlier.[24,29,30] Representative chromatograms and UV spectra are shown in Figure S1 (SI).

Identification of the Structure of Flavonoid Glucuronide. Glucuronide structures were identified using three independent methods in a sequential process as summarized in our earlier publication.[24,29−31] First, the glucuronides were hydrolyzed by β-D-glucuronidase to the aglycones. Second, the glucuronides were identified as monoglucuronides which showed a mass of (aglycone's mass + 176) Da using UPLC/MS/MS. The value 176 Da is the mass of a single attached glucuronic acid.

Finally, the sites of glucuronidation were confirmed by the UV spectrum maxima (λ_{max}) shift method.[29−31] Substitution of the 3-hydroxyl group led to a hypsochromic shift (i.e., to shorter wavelength) in band I (300−380 nm), and the shift was in the order of 13−30 nm, whereas glucuronidation of 4′-hydroxyl group produced a 5−10 nm shift. In contrast, substitution of the hydroxyl group at position C6 or C3′ had minimal or no effect on the λ_{max} of the UV spectrum (Table S2 and Figure S1, SI).

Data Analysis. Kinetic parameters were estimated by fitting the proper models (Michaelis−Menten, substrate inhibition, or Hill equations) to the substrate concentrations and initial rates with a weighting of $1/y$. Similar to glucuronidation rates, V_{max} values were also determined as nanomoles of glucuronide formed/minutes/milligrams of Supersomes protein (or nmol/mg protein/min). Eadie−Hofstee plots were used as diagnostics for model selection. Data analysis was performed by GraphPad Prism V5 for Windows (GraphPad Software, San Diego, CA). The goodness of fit was evaluated on the basis of R^2 values, RSS (residual sum of squares), rms (root-mean-square), and residual plots.

Maximal clearances (CL_{max}) were estimated using eq 1,[32,33] where V_{max} is the maximal velocity rate, S_{50} is the substrate concentration resulting in 50% of V_{max}, and n is the Hill coefficient:

$$CL_{max} = \frac{V_{max}}{S_{50}} \times \frac{n-1}{n(n-1)^{1/n}} \quad (1)$$

Correlation (Pearson) analysis was performed by GraphPad Prism V5 for Windows (GraphPad Software, San Diego, CA).

UGT1A1 and 1A9 Relative Activity Factor Determination. The relative activity factor (RAF) approach was used for scaling UGT activities obtained using cDNA-expressed enzymes to HLM.[34] RAFs (eq 2) here were defined as the HLM/recombinant enzyme activity (e.g., CL_{int}, intrinsic clearance) ratio of a particular isoform toward a probe substrate.[34]

$$RAF = \frac{CL_{int}\{probe, HLM\}}{CL_{int}\{probe, Supersome\}} \quad (2)$$

The relative amount of specific substrate metabolism attributed to an individual UGT enzyme was estimated by multiplying glucuronidation parameters (i.e., CL_{int}) observed with this enzyme by the corresponding RAF. In this study, we calculated RAFs for UGT1A1 and UGT1A9 using selective probe substrates for UGT1A1 and 1A9 (1A1: estradiol, 3-glucuronide; 1A9: propofol). Estradiol 3-glucuronidation is an excellent marker for UGT1A1, showing a good correlation with bilirubin glucuronidation.[35] Propofol is considered as an appropriate probe substrate for UGT1A9 in human liver, insomuch as a concentration of ≤100 μM (lower than K_m value) is used for activity measurement, because of the potential to be glucuronidated by other UGT isoforms.[25]

RESULTS

UGT Isoforms Involved in 3,3′,4′-THF and 3,6,4′-THF Glucuronidation. As shown in Figure 1, UGT1A1, 1A7, and 1A9 were the main isoforms glucuronidating both flavonoids. UGT1A9 showed the highest activities, followed by UGT1A1 and 1A7. In terms of the number of glucuronides formed, UGT1A7 and 1A9 only generated a single 3-*O*-glucuronide, demonstrating a strict 3-OH regioselectivity. By contrast, multiple glucuronide isomers were formed by UGT1A1 (two for 3,3′,4′-THF: 3′-*O*- and 4′-*O*-glucuronide; three for 3,6,4′-THF: 3-*O*-, 6-*O*-, and 4′-*O*-glucuronide). UGT1A7 was not considered in further studies, because it expresses only in extrahepatic tissues (i.e., stomach or esophagus).[6] We also determined the relative expression level between the 8 UGT1A isoforms by Western blot analysis using anti-UGT1A antibody (Santa Cruz Biotechnology, Santa Cruz, CA), as described previously.[29,33] There was only <1.3-fold variability in the apparent expression of the UGT1A isoforms (Figure S2, SI). Thus the UGT1A activity was not normalized using the relative expression.[33] It is acknowledged though that the interenzyme activity comparison between UGT1As and UGT2Bs might be affected by the actual enzyme levels which could not be determined due to the lack of a specific antibody for the majority of human UGT isoforms.

Contribution of UGT1A1 and 1A9 to Metabolism of 3,3′,4′-THF in pHLM. Glucuronidation kinetic profiles and constants derived from incubation of 3,3′,4′-THF with pHLM,

A

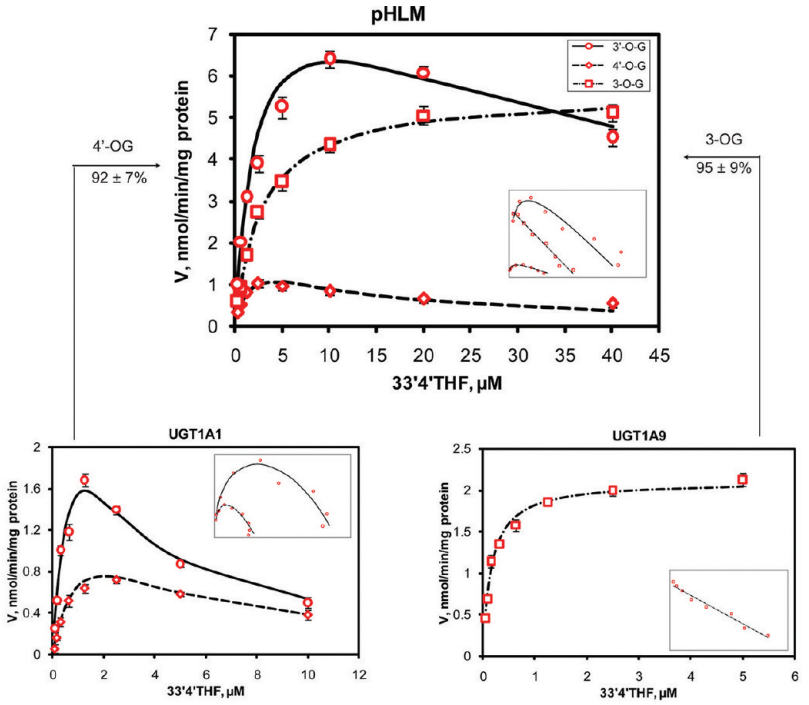

B

		V_{max}	K_m	K_{si}	CL_{int}
		nmol/min/mg protein	*μM*	*μM*	*μl/min/mg protein*
pHLM	3-OG	5.59 ± 0.10	2.87 ± 0.18	N/A	1,949 ± 123
	3'-OG	9.15 ± 1.32	2.30 ± 0.11	46.4 ± 10.1	3,981 ± 97.9
	4'-OG	1.99 ± 0.18	1.75 ± 0.09	9.25 ± 3.05	1,139 ± 68.5
UGT1A1	3'-OG	4.81 ± 0.25	1.30 ± 0.28	1.26 ± 0.45	3,075 ± 147* (77 ± 11%)
	4'-OG	1.92 ± 0.13	1.53 ± 0.34	2.61 ± 1.12	1,046 ± 57* (92 ± 7%)
UGT1A9	3-OG	2.11 ± 0.06	0.16 ± 0.01	N/A	1,846 ± 93* (95 ± 9%)

* scaled CL_{int} to pHLM using RAF approach. OG: O-glucuronidation

Figure 2. Kinetic profiles (panel A) and parameters (panel B) of glucuronidation derived from incubation of 3,3′,4′-trihydroxyflavone (3,3′,4′-THF) with pooled human liver microsomes (pHLM), recombinant UGT1A1, and UGT1A9. Insets show corresponding Eadie−Hofstee plots for each kinetic profile. Circles and solid lines denote observed and predicted formation rates of flavonoid 3′-*O*-glucuronides, respectively; diamonds and dashed lines denote observed and predicted formation rates of flavonoid 4′-*O*-glucuronides, respectively; squares and dash−dotted lines denote observed and predicted formation rates of flavonoid 3-*O*-glucuronides, respectively. Predicted rates were from Michaelis−Menten or substrate inhibition models. Each data point represents the average of three replicates. Experimental details are presented in the Experimental Section.

UGT1A1, and UGT1A9 were shown in Figure 2. The intrinsic clearance (CL_{int}) obtained with recombinant UGT1A1 and UGT1A9 were scaled to pHLM using the RAFs calculated from the UGT1A1-mediated 3-glucuronidation of estradiol (RAF = 0.83, Figure S3A, SI) and UGT1A9-mediated glucuronidation of propofol (RAF = 0.14, Figure S3B, SI). As can be seen in Figure 2, the scaled CL_{int} of UGT1A1 and UGT1A9 represented 92 ± 7% (4′-*O*-glucuronidation) and 95 ± 9% (3-*O*-glucuronidation) of the CL_{int} values in pHLM, respectively. In addition, UGT1A1 contributed a less percentage (77%) of 3′-*O*-glucuronidation in pHLM. The residual (approximately 23%) 3′-*O*-glucuronide production in pHLM might be attributable to UGT2B15, which is second most abundant in human liver[6] and showed some 3′-*O*-glucuronidation activity (Figure 1).

Contribution of UGT1A1 and 1A9 to Metabolism of 3,6,4′-THF in pHLM. Glucuronidation kinetic profiles and constants derived from incubation of 3,6,4′-THF with pHLM, UGT1A1 and UGT1A9 are shown in Figure 3. The scaled CL_{int} values of UGT1A1 and UGT1A9 accounted for 91 ± 10% (4′-*O*-glucuronidation) and 94 ± 7% (3-*O*-glucuronidation) of the CL_{int} values in pHLM, respectively. Although 3-*O*-glucuronide was primarily generated by UGT1A9, a minor contribution (9%) from UGT1A1 was also observed. For 6-*O*-glucuronide formation, a large portion (68%) was attributed to UGT1A1. However, it remains to be identified as to the other contributor(s) responsible for the remaining 32% of 6-*O*-glucuronide formation.

Expression-Activity Correlation of UGT1A1 in Human Livers. The expression levels of UGT1A1 in 12 human liver microsomes were determined by Western blot analysis (Figure 4A). In the product datasheet, it is described that the UGT1A1 antibody does not cross-react with UGT1A4, UGT1A6, UGT1A9, UGT1A10, and UGT2B15, which was also confirmed by Izukawa et al.[7] We verified that the UGT1A1 antibody did not have co-reactivity with UGT1A9 (data not shown). The variability of UGT1A1 protein in HLMs was 8.2-fold (Figure 4). The UGT1A1 protein levels were significantly correlated with the UGT1A1 activities probed with 4′-*O*-glucuronidation of 3,3′,4′-THF and 3,6,4′-THF ($R^2 > 0.811$; $p <$

A

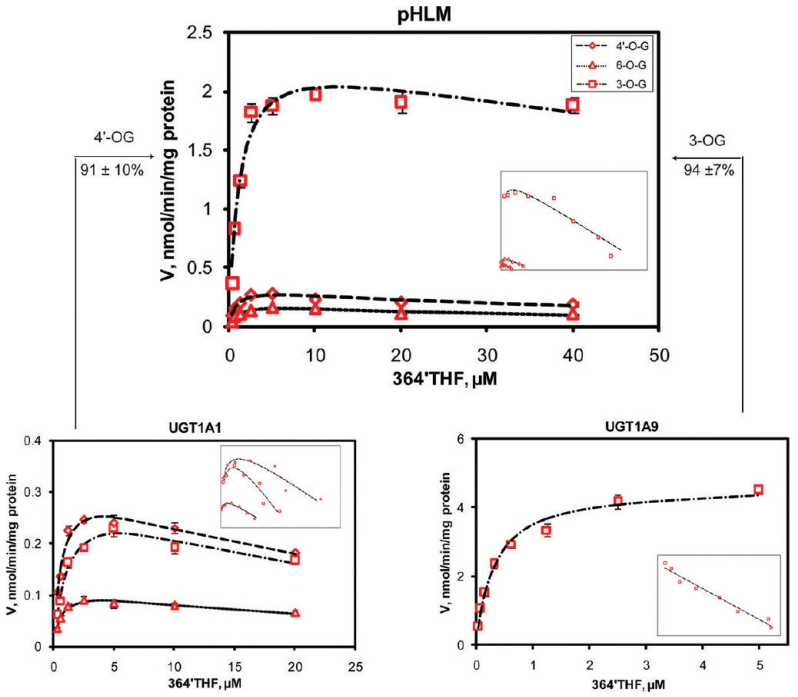

B

		V_{max}	K_m	K_{si}	CL_{int}
		nmol/min/mg protein	*μM*	*μM*	*μl/min/mg protein*
pHLM	3-OG	2.41 ± 0.19	1.16 ± 0.26	134 ± 21.2	2,082 ± 114
	6-OG	0.25 ± 0.03	1.16 ± 0.34	33.0 ± 9.22	216 ± 34
	4'-OG	0.34 ± 0.04	0.83 ± 0.23	40.0 ± 11.1	409 ± 31
UGT1A1	3-OG	0.34 ± 0.05	1.50 ± 0.40	18.9 ± 6.49	188 ± 13* (9 ± 5%)
	6-OG	0.12 ± 0.01	0.68 ± 0.13	24.4 ± 6.09	146 ± 9* (68 ± 13%)
	4'-OG	0.34 ± 0.03	0.76 ± 0.18	22.8 ± 7.22	371 ± 18* (91 ± 10%)
UGT1A9	3-OG	4.63 ± 0.16	0.33 ± 0.04	N/A	1,988 ± 176* (94 ± 7%)

* scaled CL_{int} to pHLM using RAF approach. OG: O-glucuronidation

Figure 3. Kinetic profiles (panel A) and parameters (panel B) of glucuronidation derived from the incubation of 3,6,4′-THF with pHLM, recombinant UGT1A1, and UGT1A9. Insets show corresponding Eadie−Hofstee plots for each kinetic profile. Diamonds and dashed lines denote observed and predicted formation rates of flavonoid 4′-*O*-glucuronides, respectively; triangle and dotted lines denote observed and predicted formation rates of flavonoid 6-*O*-glucuronides, respectively; squares and dash-dotted lines denote observed and predicted formation rates of flavonoid 3-*O*-glucuronides, respectively. Predicted rates were from Michaelis−Menten or substrate inhibition models. Each data point represents the average of three replicates. Experimental details are presented in the Experimental Section.

0.0001) (Figure 4B). Substantial correlations between the UGT1A1 protein and UGT1A1-mediated estradiol (3-OH) glucuronidation and SN-38 glucuronidation were also observed ($R^2 > 0.811$; $p < 0.0001$) (Figure 4C).

UGT1A1 Activity Correlation Analysis. We chose estradiol and SN-38 glucuronidation rates for correlation analysis because estradiol is the most important female hormone and also a prototypical substrate of human UGT1A1. In contrast, SN-38 is the active moiety for the widely used anticancer drug irinotecan, and UGT1A1 activities are inversely correlated to its intestinal toxicities.[11]

Highly significant correlations ($R^2 \geq 0.970$, $p < 0.0001$) were observed between rates of estradiol-3-*O*-glucuronidation and rates of 4′-*O*-glucuronidation of 3,3′,4′-THF or 3,6,4′-THF measured in a panel of HLMs ($n = 12$) (Figure S and/or Table 1). Please note that the activity correlation here was made between reaction rates measured at substrate concentrations that were lower than or near K_m (S_{50} for estradiol) values (for pHLM-mediated glucuronidation), which best approximate the intrinsic activity of a specific UGT isoform in HLMs.[36]

Glucuronidation of SN-38 in pHLM appeared to be fully (103 ± 8%) correlated with UGT1A1 activities (Figure 6A), based on the RAF approach. As expected, rates of SN-38 glucuronidation were highly correlated ($R^2 > 0.965$, $p < 0.0001$) with rates of 4′-*O*-glucuronidation of 3,3′,4′-THF or 3,6,4′-THF in the same 12 HLMs bank (Figure 6C,D and Table 1). Additionally, a similar pattern of kinetic profile (substrate inhibition) was observed between 4′-*O*-glucuronidation of 3,3′,4′-THF or 3,6,4′-THF and SN-38 glucuronidation (Figure 6B). To rule out the possibility that the observed correlations between the flavonoids and known UGT1A1 probes were due to the differences in the quality of the liver microsomes, we demonstrated that there was a lack of correlation ($p > 0.5$) between the flavonoid-4′-*O*-glucuronidation and testosterone-*O*-glucuronidation (a UGT2Bs probe)[37] in the same set of 12 HLMs (Figure S4, SI). Lastly, we confirmed that recombinant

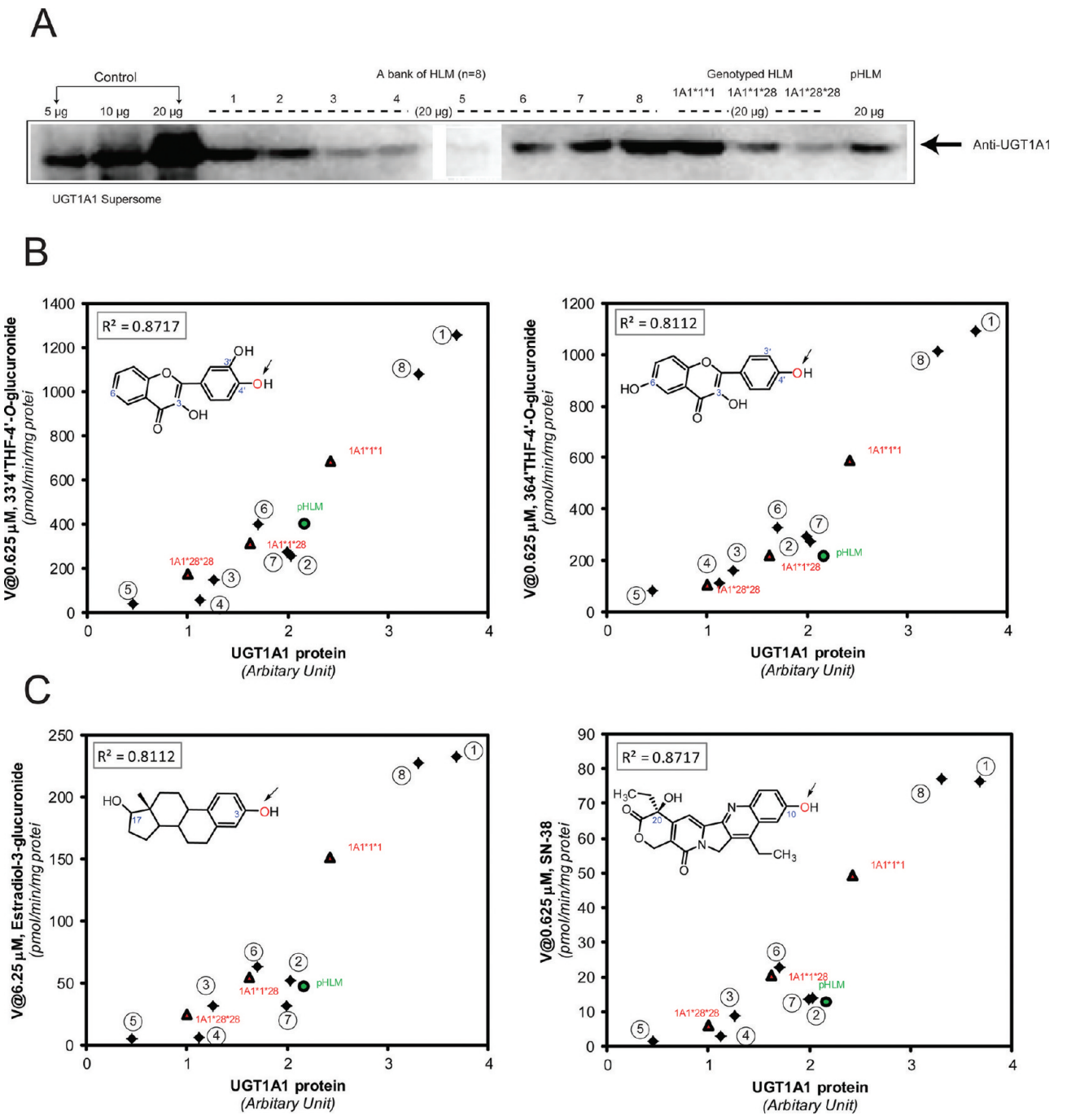

Figure 4. Western blots of recombinant UGT1A1 and human liver microsomes (panel A). Panels B–C: the correlation analyses (n = 12) were performed between the UGT1A1 protein and 3,3′,4′-THF glucuronidation (4′-OH; B, left), 3,6,4′-THF glucuronidation (4′-OH; B, right), estradiol glucuronidation (3-OH; C, left), and SN-38 glucuronidation (C, right). The eight individual HLMs from XenoTech were indicated in numbers. R^2: Pearson correlation coefficient. In panel B–C, insets show corresponding chemical structures for each UGT1A1 substrate. The arrows indicate the sites of glucuronidation.

UGT1A9 had no measurable activity toward SN-38 at lower concentrations (0.625–5 μM) and limited activity (10 ± 0.8 pmol/min/mg protein, ~5-folds less than that of UGT1A1) at a higher concentration of 10 μM, somewhat similar to the early observation.[38] Considering the fact that the *in vivo* concentration of SN-38 is quite low (<0.1 μM) after a standard therapy,[39] we believe that UGT1A9's contribution to SN-38 glucuronidation is likely to be quite limited.

DISCUSSION

We have shown that 3,3′,4′-THF and 3,6,4′-THF may be used as probe substrates for UGT1A1 because UGT1A1 displayed a high degree of selectivity toward their 4′-*O*-glucuronidation, and rates of their 4′-*O*-glucuronidation are highly correlated with UGT1A1 expression and activities in human liver microsomes. The evidence is strong and includes four sets of independent results: (1) the probes were predominantly glucuronidated (at 4′-OH) by UGT1A1 based on phenotyping of commercially available recombinant UGTs; (2) metabolism

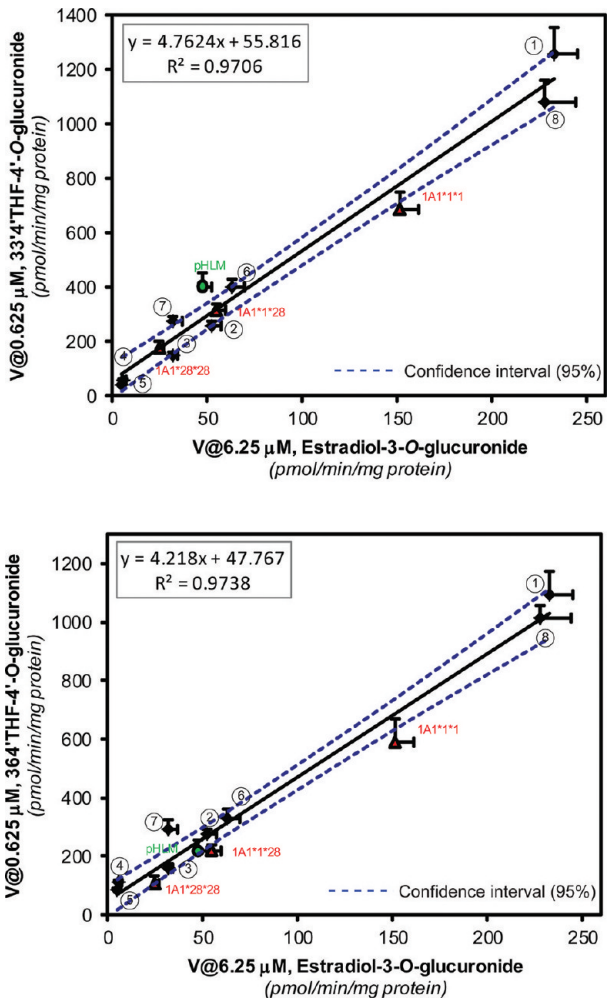

Figure 5. UGT1A1 activity correlation (R^2: Pearson correlation coefficient) between flavonoid-4′-*O*-glucuronidation (top: 3,3′,4′-THF; bottom: 3,6,4′-THF) and estradiol-3-glucuronidation in a bank of HLMs (n = 12). The eight individual HLMs from XenoTech were indicated in numbers. The borders of the 95% confidence intervals were plotted as dashed lines.

(at 4′-OH) of the probes in human liver microsomes was mainly contributed by the targeted UGT isoform; (3) the selectivity of UGT1A1 toward the flavonoid probes (4′-*O*-glucuronidation) was comparable to the known selective substrates (estradiol and SN-38) derived from activity correlation analysis; and (4) the polymorphic variants (UGT1A1*28) with decreased UGT1A1 protein expression showed markedly lower UGT1A1 activity toward the probes. Therefore, the interference of other untested hepatic isoforms (e.g., UGT2B10) on the use of the two probes was presumed to be negligible, which was supported in part by the poor correlation between 4′-*O*-glucuronidation of these two flavonoids and that of testosterone, an important substrate of UGT2Bs.

Utilities of UGT-selective probes are multifaceted in the area of glucuronidation during the drug development process.[25,28] First, they can be used to substantiate the identification of specific UGTs involved in the glucuronidation of drug candidates in human tissues via activity correlation analysis. Second, UGT-selective probes can be used to evaluate and predict the role of particular UGTs in drug−drug interactions through enzyme induction or inhibition.[26] Third, glucuronida-

Table 1. Pearson Correlation Coefficients (R^2) of Glucuronidation Reactions between 3,3′,4′-THF (4′-OH), 3,6,4′-THF (4′-OH), Estradiol (3-OH), and SN-38 in the Bank of 12 HLMs[a]

	3,3′,4′-THF V@0.625 μM	3,3′,4′-THF V@1.25 μM	3,3′,4′-THF V@2.5 μM	3,6,4′-THF V@0.625 μM	3,6,4′-THF V@1.25 μM	estradiol V@6.25 μM	estradiol V@1.25 μM	SN-38 V@0.625 μM	SN-38 V@1.25 μM
3,3′,4′-THF V@1.25 μM	0.9903								
3,3′,4′-THF V@2.5 μM	0.9733	0.9866							
3,6,4′-THF V@0.625 μM	0.9687	0.9796	0.9950						
3,6,4′-THF V@1.25 μM	0.8767[b]	0.9145	0.9471	0.9535					
Estradiol V@6.25 μM	0.9706[c]	0.9743	0.9788	0.9738[c]	0.9021				
Estradiol V@1.25 μM	0.9478	0.9506	0.9602	0.9582	0.8967	0.9926			
SN-38 V@0.625 μM	0.9657[c]	0.9687	0.9739	0.9775[c]	0.9174	0.9936	0.9893		
SN-38 V@1.25 μM	0.9687	0.9718	0.9789	0.9849	0.9224	0.9917	0.9862	0.9978	
SN-38 V@2.5 μM	0.9779	0.9820	0.9879	0.9892	0.9290	0.9907	0.9785	0.9953	0.9957

[a]The confidence of these correlations was associated with a p value of <0.0001. N = 12 for all the correlations. [b]The correlation with smallest correlation coefficient (R^2) and highest p value was chosen and presented in Figure S6 of the SI. [c]Those correlations are demonstrated in Figures 5 and 6.

dx.doi.org/10.1021/mp200300w | *Mol. Pharmaceutics* 2011, 8, 2379−2389

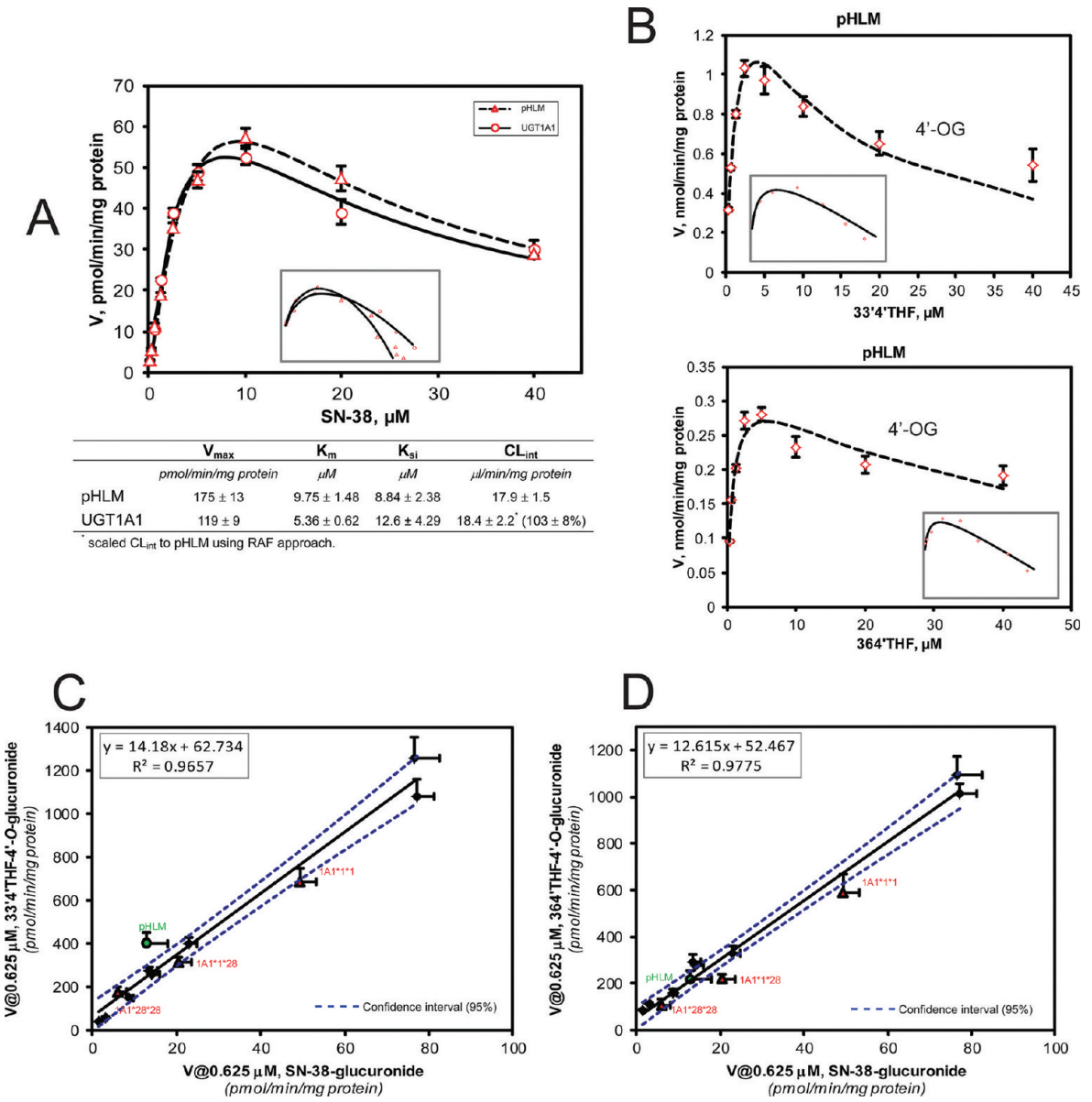

	V_{max}	K_m	K_{si}	CL_{int}
	pmol/min/mg protein	*μM*	*μM*	*μl/min/mg protein*
pHLM	175 ± 13	9.75 ± 1.48	8.84 ± 2.38	17.9 ± 1.5
UGT1A1	119 ± 9	5.36 ± 0.62	12.6 ± 4.29	18.4 ± 2.2* (103 ± 8%)

* scaled CL_{int} to pHLM using RAF approach.

Figure 6. Panel A: Kinetic profiles (top) and parameters (bottom) of glucuronidation derived from incubation of SN-38 with pHLM and recombinant UGT1A1. Panel B: Kinetic profile of 3,3′,4′-THF-4′-*O*-glucuronidation (top) and 3,6,4′-THF-4′-*O*-glucuronidation (bottom) mediated by pHLM. A similar pattern of kinetic profile (substrate inhibition) was observed between flavonoids 4′-*O*-glucuronidation and that of SN-38 glucuronidation. Panels C/D: UGT1A1 activity correlation (R^2: Pearson correlation coefficient) between flavonioid-4′-*O*-glucuronidation (C: 3,3′,4′-THF; D: 3,6,4′-THF) and SN-38 glucuronidation in a bank of HLMs (n = 12). The borders of the 95% confidence intervals were plotted as dashed lines. In panels A–B, insets show corresponding Eadie–Hofstee plots for each kinetic profile.

tion measured using UGT-selective probe in tissues from different individuals can be used as a phenotype measure to elucidate the functional significance of genetic polymorphisms.[25] Fourthly, UGT probes can be used to screen the potential inhibitors of individual UGT enzymes.[28] Finally, they can be used to establish selective functional assays to assess the functionality of individual UGT isoforms (can be reflective of metabolic status) *in vitro* (e.g., hepatocytes) and provide guidance for a clinical dosing regimen.[26,40]

Current available UGT1A1 probes are limited to three compounds: bilirubin, estradiol, and etoposide.[28] Bilirubin and estradiol are endogenous compounds, whereas etoposide is cytotoxic, precluding their use in *in vivo* glucuronidation studies. In this regard, the flavonoid probes here hold greater potential for the *in vivo* prediction of UGT1A1 activity, because they are exogenous and nontoxic.[15] As a proof of principle, UGT1A1-selective probes (*in vivo*) would be of clinical value for predicting SN-38 glucuronidation and determining the proper dose and dosing regimen.[11] SN-38 glucuronidation has been shown repeatedly to be an important factor for its gastrointestinal side effects; the deficiency in UGT1A1 activity is correlated with more severe side effects in humans.[11] It is acknowledged whether these two flavonoid probes can be used as a UGT1A1 selective probe in human remains uncertain until appropriate demonstration *in vivo*.

Interestingly, 3-*O*-glucuronidation rates of 3,3′,4′-THF and 3,6,4′-THF are also well-correlated with hepatic UGT1A9 activities as measured by the glucuronidation rates of propofol at 25 μM using the same set of HLMs (n = 12). High significant correlations ($R^2 \geq 0.944$, $p < 0.0001$) were observed

dx.doi.org/10.1021/mp200300w | *Mol. Pharmaceutics* 2011, 8, 2379–2389

between the glucuronidation of these two flavonoid probes at the 3-OH position and that of propofol (Figure S5, SI). An attempt to quantify UGT1A9 using antibodies against UGT1A9 obtained from Abnova (Taipei City, Taiwan) was unsuccessful, as the antibody cross-reacted with UGT1A1 (data not shown) and other UGT1A isoforms.[7] Therefore, we could not determine the UGT1A9 levels in human liver microsomes. This technical difficulty means that we cannot determine unequivocally if 3-*O*-glucuronidation rates of 3,3′,4′-THF and 3,6,4′-THF could be used as activity indicators for human UGT1A9, although it could be used as an indicator for glucuronidation rates of propofol, a clinically useful drug.

In addition to correlation analysis, we also used the K_m values to determine if regiospecific glucuronidation was similar in expressed UGTs and HLMs. We found that K_m values for recombinant UGT1A1 (4′-*O*-glucuronidation of 3,3′,4′-THF and 3,6,4′-THF) were essentially identical to those for pooled HLM (Figures 2 and 3), which indicated UGT1A1 was likely the predominant enzyme that catalyzed the 4′-*O*-glucuronidation. With this additional criterion, 4′-*O*-glucuronide of two flavonoids were considered the excellent markers for UGT1A1. By contrast, the K_m values for recombinant UGT1A9 (3-*O*-glucuronidation of 3,3′,4′-THF and 3,6,4′-THF) were, respectively, ∼17 (3,3′,4′-THF) and ∼2.5 (3,6,4′-THF) times lower than those for pooled HLM (Figures 2 and 3). The strikingly higher K_m value of HLM than the target recombinant UGT, as also had been found for propofol (Figure S3B of the SI)[41,42] could arise from the "membrane effect" (or "albumin effect") proposed by Miners et al.[28] It might also suggest that other UGT isoforms could contribute to the metabolism.[25] These isoforms most likely are UGT2B7 (for 3,3′,4′-THF) and UGT1A1 (for 3,6,4′-THF), inferred from the reaction-phenotyping data (Figure 1). Hence, it is necessary to reduce the low background glucuronidation activities resulted from the off-target UGTs and to use these flavonoid probes at lower concentrations (e.g., 0.625 μM for the flavonoid probes, much lower than their reported K_m values in HLMs).

It is noteworthy that the UGT1A1 expression-activity correlation did not hold between recombinant UGT1A1 and HLMs. Compared to pHLM, recombinant UGT1A1 had notably higher UGT1A1 expression in Western blot, but similar activities toward estradiol (3-glucuronide), 3,3′,4′-THF, and 3,6,4′-THF (4′-*O*-glucuronides) (Figures 2 and 3 and Figure S3, SI). The catalytic differences might be contributed by UGT protein−protein interactions (heterodimerization or hetero-oligomers) in HLMs.[43,44] There are another two possibilities that cannot be ruled out: (1) protein separation and/or binding to the membrane during Western blotting were affected by the differences in the sample matrices; (2) overexpression of UGT1A1 in insect cells may lead to the accumulation of inactive enzyme. Further studies are warranted to address this discrepancy.

In conclusion, this study presented two flavonoids (4′-*O*-glucuronidation), in which regioselective glucuronidation can be used as *in vitro* selective probes for hepatic UGT1A1, and they hold great promise for use as *in vivo* probes as well. The selectivity of UGT1A1 toward the proposed probes was systematically evaluated via studies including recombinant UGT phenotyping, individual UGT contribution estimation, and activity correlation analysis. UGT1A1 and 1A9 are the main isoforms responsible for glucuronidating 3,3′,4′-THF and 3,6,4′-THF, but at different positions (1A1, 4′-OH; 1A9, 3-OH). Glucuronidation of these two flavonoid probes at the 4′-OH position by UGT1A1 was well-correlated with estradiol-3-glucuronidation (a well-recognized and widely used UGT1A1 probe) and SN-38 glucuronidation (the drug's toxicity is associated with UGT1A1 function). The results indicated that 4′-*O*-glucuronidation of 3,3′,4′-THF and 3,6,4′-THF is excellent markers for UGT1A1 and for UGT1A1-mediated glucuronidation of SN-38. Future work should assess the selectivity of these probes in *in vivo* glucuronidation studies.

■ ASSOCIATED CONTENT

Ⓢ Supporting Information

Tables S1 and S2; Figures S1−S6. This material is available free of charge via the Internet at http://pubs.acs.org.

■ AUTHOR INFORMATION

Corresponding Author

*Mailing address: Ming Hu, Ph.D., University of Houston, Department of Pharmacological and Pharmaceutical Sciences, College of Pharmacy, 1441 Moursund Street, Houston, TX 77030. Tel.: (713)-795-8320. Fax: (713)-795-8305. E-mail: mhu@uh.edu.

■ ACKNOWLEDGMENTS

This work was supported by grants from the National Institutes of Health (GM070737) to M.H.

■ ABBREVIATIONS USED:

UGTs, UDP-glucuronosyltransferases; UPLC, ultra performance liquid chromatography; MS, mass spectroscopy; OG, O-glucuronide or O-glucuronidation; THF, trihydroxyflavone; cDNA, cDNA; HLM, human liver microsomes; pHLM, pooled human liver microsomes; RAF, relative activity factor; FDA, Food and Drug Administration

■ REFERENCES

(1) Tukey, R. H.; Strassburg, C. P. Human UDP-glucuronosyltransferases: metabolism, expression, and disease. *Annu. Rev. Pharmacol. Toxicol.* **2000**, *40*, 581−616.

(2) Kiang, T. K.; Ensom, M. H.; Chang, T. K. UDP-glucuronosyltransferases and clinical drug-drug interactions. *Pharmacol. Ther.* **2005**, *106*, 97−132.

(3) Wu, B.; Kulkarni, K.; Basu, S.; Zhang, S.; Hu, M. First-pass metabolism via UDP-glucuronosyltransferase: a barrier to oral bioavailability of phenolics. *J. Pharm. Sci.* **2011**, DOI: 10.1002/jps.22568.

(4) Gao, S.; Hu, M. Bioavailability challenges associated with development of anti-cancer phenolics. *Mini-Rev. Med. Chem.* **2010**, *10*, 550−67.

(5) Mackenzie, P. I.; Bock, K. W.; Burchell, B.; Guillemette, C.; Ikushiro, S.; Iyanagi, T.; Miners, J. O.; Owens, I. S.; Nebert, D. W. Nomenclature update for the mammalian UDP glycosyltransferase (UGT) gene superfamily. *Pharmacogenet. Genomics* **2005**, *15*, 677−685.

(6) Ohno, S.; Nakajin, S. Determination of mRNA expression of human UDP-glucuronosyltransferases and application for localization in various human tissues by real-time reverse transcriptase-polymerase chain reaction. *Drug Metab. Dispos.* **2009**, *37*, 32−40.

(7) Izukawa, T.; Nakajima, M.; Fujiwara, R.; Yamanaka, H.; Fukami, T.; Takamiya, M.; Aoki, Y.; Ikushiro, S.; Sakaki, T.; Yokoi, T. Quantitative analysis of UDP-glucuronosyltransferase (UGT) 1A and UGT2B expression levels in human livers. *Drug Metab. Dispos.* **2009**, *37*, 1759−68.

(8) Radominska-Pandya, A.; Czernik, P. J.; Little, J. M.; Battaglia, E.; Mackenzie, P.I . Structural and functional studies of UDP-glucuronosyltransferases. *Drug Metab. Rev.* **1999**, *31*, 817−899.

(9) Emoto, C.; Murayama, N.; Rostami-Hodjegan, A.; Yamazaki, H. Methodologies for Investigating Drug Metabolism at the Early Drug Discovery Stage: Prediction of Hepatic Drug Clearance and P450 Contribution. *Curr. Drug Metab.* **2010**, *11*, 678−85.
(10) Fujita, K.; Sparreboom, A. Pharmacogenetics of irinotecan disposition and toxicity: a review. *Curr. Clin. Pharmacol.* **2010**, *5*, 209−17.
(11) O'Dwyer, P. J.; Catalano, R. B. Uridine diphosphate glucuronosyltransferase (UGT) 1A1 and irinotecan: practical pharmacogenomics arrives in cancer therapy. *J. Clin. Oncol.* **2006**, *24*, 4534−8.
(12) Beutler, E.; Gelbart, T.; Demina, A. Racial variability in the UDP-glucuronosyltransferase 1 (UGT1A1) promoter: a balanced polymorphism for regulation of bilirubin metabolism? *Proc. Natl. Acad. Sci. U.S.A.* **1998**, *95*, 8170−8174.
(13) Crozier, A.; Jaganath, I. B.; Clifford, M. N. Dietary phenolics: chemistry, bioavailability and effects on health. *Nat. Prod. Rep.* **2009**, *26*, 1001−43.
(14) Jeong, E. J.; Liu, X.; Jia, X.; Chen, J.; Hu, M. Coupling of conjugating enzymes and efflux transporters: impact on bioavailability and drug interactions. *Curr. Drug Metab.* **2005**, *6*, 455−68.
(15) Hu, M. Commentary: bioavailability of flavonoids and polyphenols: call to arms. *Mol. Pharmaceutics* **2007**, *4*, 803−6.
(16) Joseph, T. B.; Wang, S. W.; Liu, X.; Kulkarni, K. H.; Wang, J.; Xu, H.; Hu, M. Disposition of flavonoids via enteric recycling: enzyme stability affects characterization of prunetin glucuronidation across species, organs, and UGT isoforms. *Mol. Pharmaceutics* **2007**, *4*, 883−894.
(17) Tang, L.; Singh, R.; Liu, Z.; Hu, M. Structure and Concentration Changes Affect Characterization of UGT Isoform-Specific Metabolism of Isoflavones. *Mol. Pharmaceutics* **2009**, *6*, 1466−1482.
(18) Tang., L.; Ye, L.; Singh, R.; Wu, B.; Lv, C.; Zhao, J.; Liu, Z.; Hu, M. Use of Glucuronidation Fingerprinting to Describe and Predict mono- and di- Hydroxyflavone Metabolism by Recombinant UGT Isoforms and Human Intestinal and Liver Microsomes. *Mol. Pharmaceutics* **2010**, *7*, 664−79.
(19) Zhou, Q.; Zheng, Z.; Xia, B.; Tang, L.; Lv, C.; Liu, W.; Liu, Z.; Hu, M. Use of isoform-specific UGT metabolism to determine and describe rates and profiles of glucuronidation of wogonin and oroxylin A by human liver and intestinal microsomes. *Pharm. Res.* **2010**, *27*, 1568−83.
(20) Chen, Y. K.; Chen, S. Q.; Li, X.; Zeng, S. Quantitative regioselectivity of glucuronidation of quercetin by recombinant UDP-glucuronosyltransferases 1A9 and 1A3 using enzymatic kinetic parameters. *Xenobiotica* **2005**, *35*, 943−954.
(21) Lépine, J.; Bernard, O.; Plante, M.; Têtu, B.; Pelletier, G.; Labrie, F.; Bélanger, A.; Guillemette, C. Specificity and regioselectivity of the conjugation of estradiol, estrone, and their catecholestrogen and methoxyestrogen metabolites by human uridine diphospho-glucuronosyltransferases expressed in endometrium. *J. Clin. Endocrinol. Metab.* **2004**, *89*, 5222−32.
(22) Brill, S. S.; Furimsky, A. M.; Ho, M. N.; Furniss, M. J.; Li, Y.; Green, A. G.; Bradford, W. W.; Green, C. E.; Kapetanovic, I. M.; Iyer, L. V. Glucuronidation of trans-resveratrol by human liver and intestinal microsomes and UGT isoforms. *J. Pharm. Pharmacol.* **2006**, *58*, 469−79.
(23) Ohno, S.; Kawana, K.; Nakajin, S. Contribution of UDP-glucuronosyltransferase 1A1 and 1A8 to morphine-6-glucuronidation and its kinetic properties. *Drug. Metab. Dispos.* **2008**, *36*, 688−94.
(24) Wu, B.; Morrow, J. K.; Singh, R.; Zhang, S.; Hu, M. 3D-QSAR Studies on UGT1A9-mediated 3-O-Glucuronidation of Natural Flavonols Using a Pharmacophore-based CoMFA Model. *J. Pharmacol. Exp. Ther.* **2011**, *336*, 403−13.
(25) Court, M. H. Isoform-selective probe substrates for in vitro studies of human UDP-glucuronosyltransferases. *Methods Enzymol.* **2005**, *400*, 104−16.
(26) Donato, M. T.; Montero, S; Castell, J. V.; Gómez-Lechón, M. J.; Lahoz, A. Validated assay for studying activity profiles of human liver UGTs after drug exposure: inhibition and induction studies. *Anal. Bioanal. Chem.* **2010**, *396*, 2251−63.
(27) Stone, A. N.; Mackenzie, P. I.; Galetin, A.; Houston, J. B.; Miners, J. O. Isoform selectivity and kinetics of morphine 3- and 6-glucuronidation by human UDP-glucuronosyltransferases: evidence for atypical glucuronidation kinetics by UGT2B7. *Drug Metab. Dispos.* **2003**, *31*, 1086−9.
(28) Miners, J. O.; Mackenzie, P. I.; Knights, K. M. The prediction of drug-glucuronidation parameters in humans: UDP-glucuronosyltransferase enzyme-selective substrate and inhibitor probes for reaction phenotyping and in vitro-in vivo extrapolation of drug clearance and drug-drug interaction potential. *Drug Metab. Rev.* **2010**, *42*, 189−201.
(29) Wu, B.; Xu, B.; Hu, M. Regioselective Glucuronidation of Flavonols by Six Human UGT1A Isoforms. *Pharm. Res.* **2011**, *28* (8), 1905−18.
(30) Singh, R.; Wu, B.; Tang, L.; Hu, M. Uridine Diposphate Glucuronosyltransferases Isoform-Dependent Regiospecificity of Glucuronidation of Flavonoids. *J. Agric. Food. Chem.* **2011**, *59* (13), 7452−64.
(31) Singh, R.; Wu, B.; Tang, L.; Liu, Z.; Hu, M. Identification of the Position of Mono-O-Glucuronide of Flavones and Flavonols by Analyzing Shift in Online UV Spectrum (λ_{max}) Generated from an Online Diode-arrayed Detector. *J. Agric. Food Chem.* **2010**, *58*, 9384−95.
(32) Houston, J. B.; Kenworthy, K. E. In vitro-in vivo scaling of CYP kinetic data not consistent with the classical Michaelis-Menten model. *Drug Metab. Dispos.* **2000**, *28*, 246−54.
(33) Uchaipichat, V.; Mackenzie, P. I.; Guo, X. H.; Gardner-Stephen, D.; Galetin, A.; Houston, J. B.; Miners, J. O. Human UDP-glucuronosyltransferases: isoform selectivity and kinetics of 4-methylumbelliferone and 1-naphthol glucuronidation, effects of organic solvents, and inhibition by diclofenac and probenecid. *Drug Metab. Dispos.* **2004**, *32*, 413−23.
(34) Rouguieg, K.; Picard, N.; Sauvage, F. L.; Gaulier, J,M.; Marquet, P. Contribution of the different UDP-glucuronosyltransferase (UGT) isoforms to buprenorphine and norbuprenorphine metabolism and relationship with the main UGT polymorphisms in a bank of human liver microsomes. *Drug. Metab. Dispos.* **2010**, *38*, 40−5.
(35) Zhou, J.; Tracy, T. S.; Remmel, R. P. Correlation between Bilirubin Glucuronidation and Estradiol-3-Gluronidation in the Presence of Model UGT1A1 Substrates/Inhibitors. *Drug. Metab. Dispos.* **2011**, *39*, 322−9.
(36) Zhang, D.; Zhang, D.; Cui, D.; Gambardella, J.; Ma, L.; Barros, A.; Wang, L.; Fu, Y.; Rahematpura, S.; Nielsen, J.; Donegan, M.; Zhang, H.; Humphreys, W. G. Characterization of the UDP glucuronosyltransferase activity of human liver microsomes genotyped for the UGT1A1*28 polymorphism. *Drug Metab. Dispos.* **2007**, *35*, 2270−80.
(37) Sten, T.; Bichlmaier, I.; Kuuranne, T.; Leinonen, A.; Yli-Kauhaluoma, J.; Finel, M. UDP-glucuronosyltransferases (UGTs) 2B7 and UGT2B17 display converse specificity in testosterone and epitestosterone glucuronidation, whereas UGT2A1 conjugates both androgens similarly. *Drug Metab. Dispos.* **2009**, *37*, 417−23.
(38) Hanioka, N.; Ozawa, S.; Jinno, H.; Ando, M.; Saito, Y.; Sawada, J. Human liver UDP-glucuronosyltransferase isoforms involved in the glucuronidation of 7-ethyl-10-hydroxycamptothecin. *Xenobiotica* **2001**, *31*, 687−99.
(39) Mathijssen, R. H.; van Alphen, R. J.; Verweij, J.; Loos, W. J.; Nooter, K.; Stoter, G.; Sparreboom, A. Clinical pharmacokinetics and metabolism of irinotecan (CPT-11). *Clin. Cancer Res.* **2001**, *7*, 2182−94.
(40) Bonora-Centelles, A.; Donato, M. T.; Lahoz, A.; Pareja, E.; Mir, J.; Castell, J. V.; Gómez-Lechón, M. J. Functional characterization of hepatocytes for cell transplantation: customized cell preparation for each receptor. *Cell. Transplant* **2010**, *19*, 21−8.
(41) Soars, M. G.; Ring, B. J.; Wrighton, S. A. The effect of incubation conditions on the enzyme kinetics of udp-glucuronosyltransferases. *Drug Metab. Dispos.* **2003**, *31*, 762−7.

(42) Shimizu, M.; Matsumoto, Y.; Yamazaki, H. Effects of propofol analogs on glucuronidation of propofol, an anesthetic drug, by human liver microsomes. *Drug Metab. Lett.* **2007**, *1*, 77−9.
(43) Fujiwara, R.; Nakajima, M.; Oda, S.; Yamanaka, H.; Ikushiro, S.; Sakaki, T.; Yokoi, T. Interactions between human UDP-glucuronosyltransferase (UGT) 2B7 and UGT1A enzymes. *J. Pharm. Sci.* **2010**, *99*, 442−54.
(44) Fujiwara, R.; Nakajima, M.; Yamanaka, H.; Katoh, M.; Yokoi, T. Interactions between human UGT1A1, UGT1A4, and UGT1A6 affect their enzymatic activities. *Drug Metab. Dispos.* **2007**, *35*, 1781−7.